Photoactivation

DOI: 10.1002/anie.201410940

Design of Photocaged Puromycin for Nascent Polypeptide Release and Spatiotemporal Monitoring of Translation**

*Florian Buhr, Jörg Kohl-Landgraf, Susanne tom Dieck, Cyril Hanus, Deep Chatterjee, Andreas Hegelein, Erin M. Schuman, Josef Wachtveitl, and Harald Schwalbe**

Abstract: *The antibiotic puromycin, which inhibits protein translation, is used in a broad range of biochemical applications. The synthesis, characterization, and biological applications of NVOC-puromycin, a photocaged derivative that is activated by UV illumination, are presented. The caged compound had no effect either on prokaryotic or eukaryotic translation or on the viability of HEK 293 cells. Furthermore, no significant release of ribosome-bound polypeptide chains was detected in vitro. Upon illumination, cytotoxic activity, in vitro translation inhibition, and polypeptide release triggered by the uncaging of NVOC-puromycin were equivalent to those of the commercial compound. The quantum yield of photolysis was determined to be 1.1 ± 0.2 % and the NVOC-puromycin was applied to the detection of newly translated proteins with remarkable spatiotemporal resolution by using two-photon laser excitation, puromycin immunohistochemistry, and imaging in rat hippocampal neurons.*

The antibiotic agent puromycin (**1**), which was first isolated from the gram-positive bacterium *Streptomyces alboniger,* is a well-studied inhibitor of translation with a wide variety of biochemical applications.[1] Puromycin enters the ribosomal A site during translation, where it acts as a codon-unspecific competitor of aminoacyl-tRNA as a result of its structural similarity to the 3′ end of tyrosyl-tRNA.[2,3] Upon nucleophilic attack, the C terminus of the nascent polypeptide chain is transferred from the 3′ end of the peptidyl-tRNA located at the ribosomal P-site near the peptidyl transferase center (PTC) to the amino group of puromycin.[4–6] The newly formed peptidyl-puromycin is resistant to cleavage by the PTC, thus resulting in premature chain termination and subsequent release from the ribosome on a subsecond timescale.[7–9]

Puromycin and a number of synthetic derivatives have been used as PTC substrate analogues to gain insights into peptide bond formation.[8–15] Unlike other methods for nascent polypeptide release, such as treatment with RNase A/EDTA or NaOH, the use of puromycin does not cause ribosomal particles to disintegrate and nor does it induce the formation of insoluble aggregates.[7] In many experiments, nascent polypeptide chain release is induced by puromycin,[16] and at low concentrations, it can be used to identify translating ribosomes,[17] to purify newly synthesized polypeptide chains and associated chaperones,[18] or to monitor translation. Chemically modified versions of puromycin are common as well. In mRNA display, covalently bound puromycin facilitates the attachment of an mRNA progenitor to its respective peptide product[19] and in TRAP display,[20] a puromycin-coupled DNA linker is hybridized with mRNAs, while fluorescent puromycin conjugates have been used to identify nascent polypeptide chains in vivo.[17] More recently, biotinylated puromycin was used for puromycin-associated nascent chain proteomics (PUNCH-P) to monitor translation on a proteomic scale.[21]

In order to allow spatiotemporal control of the application of puromycin for biophysical and cellular studies, a photocaged derivative of puromycin was synthesized and characterized. The principal utility of photocaged antibiotics as light-activated effectors has been demonstrated previously. Photocaged rapamycin has been used to induce activity of the small GTPase Rac in a cellular context[22] and photocaged anisomycin has been used to locally inhibit protein synthesis.[23] In the case of puromycin, however, the scope of its biological applications is much wider owing to its unique mode of action and would be further extended by biologically compatible light-activation. The well-established 6-nitroveratryloxycarbonyl (NVOC) photolabile protecting group,[24–26] which was used in this study, meets critical requirements for compatibility with biological systems: sufficient water solubility, low cytotoxicity, high dark stability, and moderate ambient light tolerance, as well as an uncaging wavelength beyond the absorption range of common biomolecules.

NVOC-puromycin **2** (Figure 1) was obtained in 59 % yield in a one-step synthesis followed by reversed-phase HPLC purification. Dissolved in DMSO or H_2O, the caged compound is stable in the dark for at least 48 h at room temperature or for at least 6 months at −20 °C. Although the protection of its protonatable amino group dramatically

[*] F. Buhr, D. Chatterjee, A. Hegelein, Prof. Dr. H. Schwalbe
Center for Biomolecular Magnetic Resonance
Institute of Organic Chemistry and Chemical Biology
Goethe-Universität Frankfurt am Main
Max-von-Laue-Straße 7, 60438 Frankfurt am Main (Germany)
E-mail: schwalbe@nmr.uni-frankfurt.de
J. Kohl-Landgraf, Prof. Dr. J. Wachtveitl
Institute of Physical and Theoretical Chemistry
Goethe-Universität Frankfurt am Main
Max-von-Laue-Straße 7, 60438 Frankfurt am Main (Germany)
S. tom Dieck, C. Hanus, Prof. Dr. E. M. Schuman
Department of Synaptic Plasticity, MPI for Brain Research
Max-von-Laue-Straße 4, 60438 Frankfurt am Main (Germany)

[**] We thank E. Stirnal, B. Fürtig, F. Sochor, M. Strumpf, R. Silvers and C. Richter for support. This work was funded by the DFG in Collaborative Research Center SFB807 and the HFSP. H.S. and J.W. are members of the cluster of excellence: Macromolecular Complexes.

Supporting information for this article is available on the WWW under http://dx.doi.org/10.1002/anie.201410940.

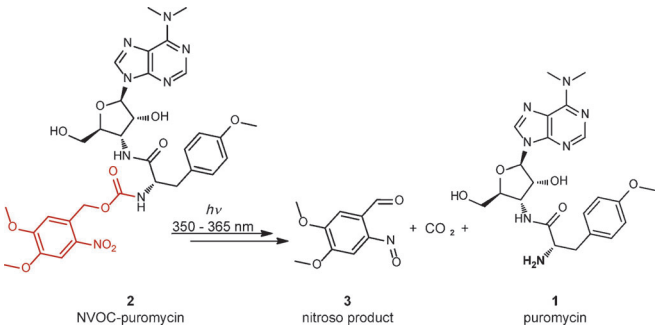

Figure 1. Constitution and uncaging of NVOC-puromycin. The nitroveratryloxycarbonyl protecting group is shown in red. During uncaging, puromycin is released by decarboxylation, with formation of the final nitroso caging remnant **3**.

reduces polarity, the remaining water solubility of 2.5 mM (20 °C) exceeds the required concentrations in cell culture selection media by three orders of magnitude.[27,28] Upon UV illumination above 320 nm, puromycin was recovered as confirmed by ^{1}H NMR spectroscopy and mass spectrometry. Optimization for biochemical applications requires the photochemical characterization of the uncaging reaction, in which quantum yield is the most critical parameter since it reflects the expected amount of released puromycin after a given illumination time. To determine the quantum yield, we monitored the development of the nitroso absorption under continuous UV irradiation (Figure 1, Figure 2a). To simplify analysis, we only took into account the first 120 seconds of this experiment, during which the exponential behavior can be approximated by a linear function (Figure 2b). In this case, we can assume that all photons are absorbed only by the reactant and not by the product since the amount of product formed within the investigated time range is negligible. Furthermore, the absorbance change around 410 nm is caused by the product only and can thus be directly used to determine the number of total photoreactions. With these considerations, we obtained a quantum yield of $1.1 \pm 0.2\,\%$. The results of a second approach, which was based on the IR absorption of soluble CO_2, are presented in the Supporting Information, along with the derivation of both methods.

Although a number of different caging groups are conceivable, we decided to introduce the 6-nitroveratryloxycarbonyl group. For NVOC-puromycin, the electron-donating substitutions necessary to shift the absorption to a biologically compatible wavelength result in a reduction in quantum efficiency via a nonreactive triplet-state trap in the uncaging mechanism.[29] Despite this drawback, the NVOC group has notable advantages over more recently established photocages with superior photochemical characteristics. NVOC chloride is commercially available and can be used directly in a one-pot synthesis, whereas there is currently no commercial access to the widely used coumarin-based chloroformiates. Additionally, since the uncaging reaction proceeds through a singlet pathway,[29] the absence of radical intermediates might be beneficial for applications in vivo, where the quenching of reactive triplet states by cellular radicals should be avoided. To determine the available concentration

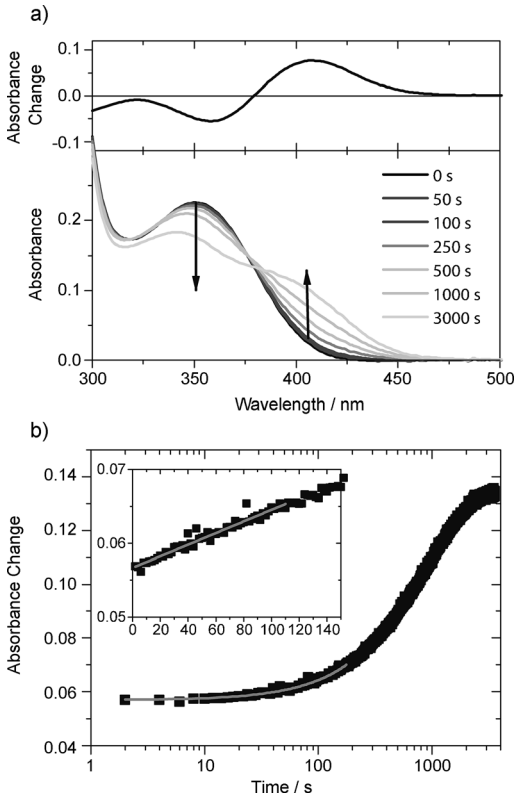

Figure 2. Quantum yield and uncaging kinetics determined by absorption of the nitroso caging remnant. a) Lower panel: Absorption spectra of the caged compound (black curve) and after various irradiation intervals with an intensity of 7 mW at 365 nm (gray curves). Upper panel: Difference spectrum of the sample after 3000 s of continuous irradiation. b) Absorbance at 410 nm during continuous UV irradiation on a logarithmic time scale. The inset shows the linear time range that was used for the fit. In both graphs, the thin grey curve shows the linear fit curve.

of uncaged puromycin after increasing periods of illumination in a practical setup of interest, an interval series of laser-coupled ^{1}H NMR experiments[30] was performed, in which a molar excess of free puromycin with respect to common antibiotic concentrations or concentrated prokaryotic ribosomes was reached on a low second timescale (see the Supporting Information).

To assess the deactivation and recovery of the cytotoxic effect, cultures of human embryonic kidney (HEK) 293 cells were incubated with caged, uncaged, or commercial puromycin. Uncaging was achieved by illumination with a 365 nm LED, operated at 200 mW. After 24 h of incubation at 37 °C, an XTT cell viability assay was performed to evaluate the number of viable cells. The assay exploits the activity of mitochondrial dehydrogenase since this correlates with the number of metabolically active cells. The results for the caged compound did not differ from those obtained with negative controls, thus showing that NVOC-puromycin has no significant toxicity and remains stable under cell culture conditions (Figure 3a). However, the effect of previously illuminated NVOC-puromycin was equivalent to that of the commercial compound, corresponding to a complete recovery of cytotoxic function after uncaging. In a further experiment, cell culture

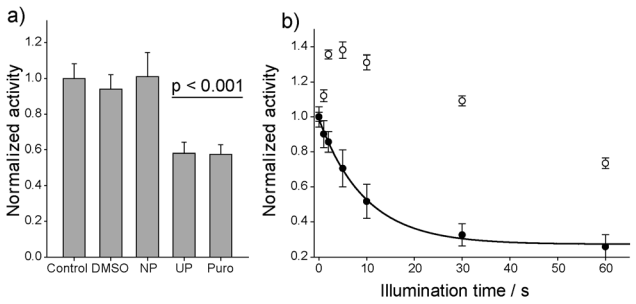

Figure 3. XTT cell viability assays with treated HEK 293 cells. a) HEK 293 cells treated with 6.3 μM NVOC-puromycin (NP), uncaged puromycin (UP), or commercial puromycin (Puro) were incubated at 37 °C for 24 h. Control experiments contained no additive or 0.1 % DMSO. Error bars represent one standard deviation and were calculated from ten parallel experiments performed for each data point. The p-value refers to all pairs of Control/DMSO/CP vs. UP/Puro. b) Filled circles: HEK 293 cells were treated with 6.3 μM NVOC-puromycin and aliquots were illuminated at 365 nm for increasing periods of time. All samples were incubated at 37 °C for 24 h before the XTT assay was performed. Empty circles: Negative control without NVOC-puromycin. All illumination experiments were performed in triplicate.

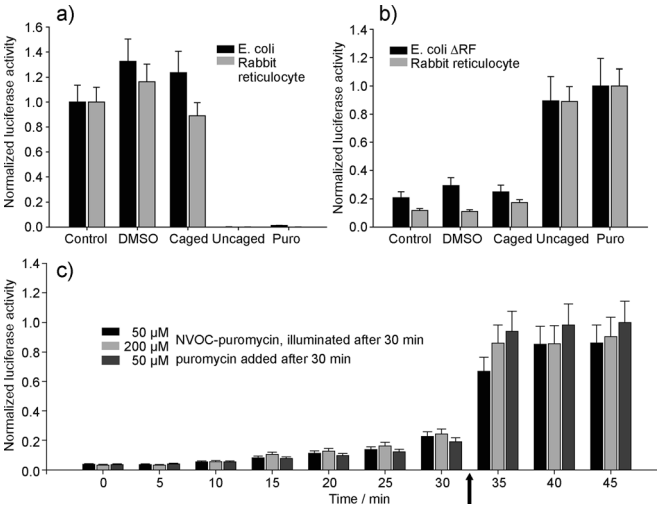

Figure 4. Firefly luciferase expression assays. a) Expression in two different in vitro systems, where luciferase activity after 1 h of incubation with 50 μM caged, uncaged, or commercial puromycin was compared. b) Expression in a reconstituted *E. coli* system lacking release factors (black) or with a DNA template lacking a stop codon in a rabbit reticulocyte system (gray). c) In a time-dependent interval experiment, samples were incubated with NVOC-puromycin (black and pale gray) or with no added compound (dark grey) as a control. Luciferase activity was detected in samples taken every 5 min until 30 min, at which point the cell-free reactions treated with NVOC-puromycin were illuminated at 365 nm for 1 min (black arrow) and puromycin was added to the control samples. Error bars represent one standard deviation and were calculated from triplicate measurements for each data point.

aliquots with and without previous addition of the caged compound were illuminated for increasing periods of time. As shown in Figure 3b, the addition of NVOC-puromycin causes cell viability measured after 24 h to decay exponentially with illumination time. While no net decay caused by UV exposure alone was detected after up to 30 s (Figure 3), 95 ± 1 % of the maximum effect was achieved in the same period with NVOC-puromycin. A time constant (τ) of 9.7 ± 0.6 s was obtained under the given experimental conditions, which corresponds to 25 ± 1 % of the maximum effect observed in less than 3 s. This result implies that with an easily accessible tenfold increase in initial concentration (63 μM), full cytotoxic efficiency is achieved after 1 s of illumination. Since an initial increase in cell viability is observed in the negative control, UV illumination seems to have multiple effects. Cytotoxicity however, was shown to be negligible in the given time frame.

To demonstrate the inhibition of in vitro translation, firefly luciferase expression assays were performed by using an *E. coli* extract based expression system and a rabbit reticulocyte cell-free expression system. The addition of 50 μM of uncaged NVOC-puromycin or commercial puromycin completely inhibits translation (Figure 4a), while the caged compound shows no inhibitory effect compared to the DMSO control. In the early days of co-translational protein folding research, it was concluded that nascent polypeptide chains of firefly luciferase had to be partially folded, but were catalytically inactive while ribosome-bound.[34] This feature was exploited in a modified luciferase assay, in which arrested ribosomes with inactive luciferase chains covalently attached to the tRNA at the P-site were generated. Puromycin-mediated release of the nascent chain thus induces an amount of enzyme activity equivalent to a single round of translation with the excess puromycin preventing further translation. Experiments were performed using two different expression systems. First, a PCR-generated run-off template was expressed in an *E. coli* system reconstituted from purified components and lacking release factors. Second, a truncated template without a stop codon was expressed in a rabbit reticulocyte system. Figure 4b shows normalized luciferase activity of the expressed constructs before (control) and after the addition of caged, uncaged, or commercial puromycin. The base level of activity caused by leak release is exceeded four- to five-fold by puromycin-mediated release of the ribosome-bound population. The difference observed between the effects of commercial versus uncaged puromycin are within experimental error, although it is conceivable that for the caged compound, adjusted starting concentrations may be required to recover an equivalent effect by uncaging, especially if illumination time is limiting. In a further experiment, luciferase activity was measured every 5 min during the expression of ribosome-bound luciferase with added NVOC-puromycin. After 30 min, reactions were illuminated for 1 min and three more data points were measured. In a control reaction with no added compound, commercial puromycin (50 μM) was introduced at the 30 min time point. A minor but steady increase in enzyme activity is observed before illumination because of leak release (Figure 4c). In all three cases, the luciferase-activating effect of puromycin-mediated release from the ribosome after illumination or puromycin addition at 30 min was comparable, with the differences being within experimental error. A significant difference between the uncaging of the 50 μM and 200 μM NVOC-puromycin reaction was only detected at the first data point after uncaging (35 min), thus suggesting slow release kinetics as

a result of insufficient concentrations of the free compound. Since the concentration of ribosomes in cell-free extracts does not exceed the lower μM range, a molar excess of uncaged puromycin accumulates rapidly upon illumination, given sufficient starting concentrations and illumination conditions.

At low concentrations, puromycin has previously been used to monitor protein translation.[17,32,33] In the next series of experiments, we aimed to introduce spatiotemporal control to the puromycin-mediated monitoring of newly translated proteins. First, we showed illumination dependence of nascent chain puromycylation in cultures of rat hippocampal neurons when incubated with 3 μM NVOC-puromycin, both by Western blotting (Figure 5a) and immunocytochemistry (Figure 5b). As expected, labelling of cells treated with commercial puromycin was roughly equal in the presence or absence of illumination. By contrast, in cells exposed to NVOC-puromycin, puromycylation was only observed after illumination (Figure 5a). Interestingly, illumination-dependent puromycylation, albeit to a lower extent, was also observed after preincubation (30 min/60 min) of the cells with NVOC-puromycin, followed by washes to remove extracellular NVOC-puromycin before illumination (±) and a 10 min incorporation period, thus indicating that the caged compound is also taken up, albeit with slower kinetics than puromycin. Nonetheless this fact allowed us to spatially restrict puromycylation by simply adding an illumination mask. The first spatial control experiment was performed by using an aperture that allowed partial illumination of the cell culture dish (Figure 5c) after preincubation of the entire dish with 3 μM NVOC-puromycin for 30 min and washing before a 60 s illumination period. Puromycylation inside the illuminated inner area compared to the non-illuminated outer area was equivalent to the results for NVOC-puromycin with and without illumination, thus demonstrating that simple spatial control can be achieved through selective illumination within a single cell culture dish.

To dramatically increase spatial resolution, GFP-transfected neurons were incubated with 3 μM NVOC-puromycin for 30 min and a single cell was illuminated by using a two-photon laser at 720 nm in two 1.6 × 1.6 μm regions of interest (8 × 8 pixels, 5 ms illumination per pixel, 10 times in one minute intervals, Figure 5d, upper left inset). To detect puromycylation, dishes were processed for puromycin immunocytochemistry 10 min after the first laser pulse. Imaging of illuminated versus non-illuminated transfected and non-transfected cells in the same dishes revealed that puromycylation of newly translated proteins was detected with surprising spatial precision. Puromycin signal above background was only detected in the illuminated cell and the intensity was highest within a narrow strip around the illumination spots, whereas only a faint background signal was detected in non-illuminated cells.

In summary, we present the synthesis of a photocaged puromycin derivative and its biophysical and biochemical characterization. By using NVOC as photolabile protecting group, we demonstrated photoinducible toxicity to eukaryotic cells, as well as the inhibition of protein translation in vitro in prokaryotic and eukaryotic cell-free expression systems. We further showed that triggered polypeptide chain release can

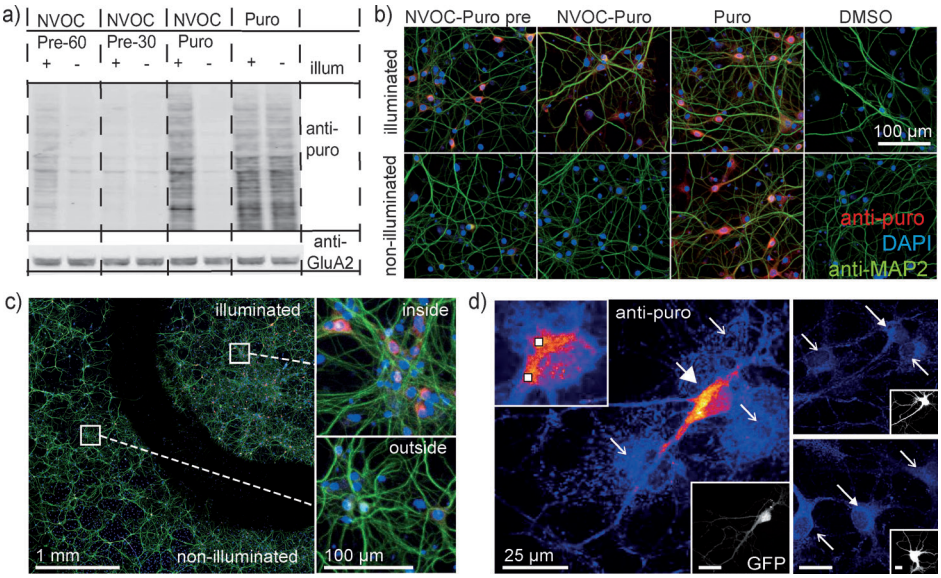

Figure 5. Puromycylation of nascent protein chains in rat hippocampal neurons. a) Western blot of lysed cells probed with a primary anti-puromycin antibody. NVOC Pre-60/30: preincubated with 3 μM NVOC-puromycin for 60/30 min followed by 3 washing steps. NVOC-Puro: 3 μM NVOC-puromycin. Puromycin: 3 μM commercial puromycin. Treated cells were subjected to illumination (+) or no illumination (−) for 30 s followed by a 10 min incorporation period. Loading control: Anti-GluA2. Negative control: Cells incubated with DMSO (not shown). Lane intensity analysis in Figure S4 in the Supporting Information. b) Microscopic immunocytochemistry images of hippocampal neurons stained with an anti-puromycin antibody (red), DAPI (nucleus, blue), and an anti-MAP2 antibody (dendrites, green). Culture dishes were incubated as described for the Western Blot and cells with or without illumination were processed for puromycin immunocytochemistry. The preincubation time was 30 min and the illumination time was 60 s. c) Simple spatial control experiment using aperture illumination with a circular mask. Experimental conditions were otherwise identical to the pre-incubated sample in (b). The white boxes represent the zoomed micrographs on the right. The position of the illumination mask on the culture dish was circled using a black marker (dark trail). d) Cells after two-photon uncaging of NVOC-puromycin at two spots in a single, transfected neuron per dish. The whole dish was processed for puromycin immunohistochemistry and the illuminated cell and other cells in the dish were identified based on the transfection marker (GFP) and shape (lower right insets). Right panels: non-illuminated transfected control cells after incubation (transfected cells, filled arrowheads; non-transfected cells, line arrows). Neither non-illuminated, transfected cells nor the surrounding non-transfected cells show significant puromycin incorporation. Left panel: puromycin signal following two-photon uncaging inside the cell body of an illuminated neuron. The localization of the two illumination regions is indicated by white squares (top left inset).

be achieved in vitro. Lastly, we demonstrated the use of NVOC-puromycin to spatially control the release and incorporation of puromycin into living cells. Since local synthesis of proteins near neuronal synapses is thought to be one of the key mechanisms involved in the cellular expression of learning and memory,[34] the spatiotemporal monitoring of protein synthesis and the identification of these newly synthesized proteins is a task of utmost importance. Puromycylation is a powerful mechanism for tagging nascent proteins. The demonstrated illumination-dependent spatiotemporal control of puromycin application in combination with living neurons promises an exciting approach to accomplish this task. Localized translation plays a much wider role than in just learning and memory and has been shown in a multitude of systems.[34,35] We conclude that photocaged puromycin will be of great use for numerous existing and new biological applications.

Received: November 13, 2014
Revised: November 26, 2014
Published online: February 4, 2015

Keywords: antibiotics · inhibitors · photoactivation · protecting groups · protein expression

[1] C. Waller, P. Fryth, *J. Am. Chem. Soc.* **1953**, *75*, 2025.
[2] J. D. Smith, R. R. Traut, G. M. Blackburn, R. E. Monro, *J. Mol. Biol.* **1965**, *13*, 617 – 628.
[3] D. Allen, P. Zamecnik, *Biochim. Biophys. Acta* **1962**, *55*, 865 – 874.
[4] D. Nathans, *Proc. Natl. Acad. Sci. USA* **1964**, *51*, 585 – 592.
[5] A. Morris, S. Favelukes, *Biochem. Biophys. Res. Commun.* **1962**, *7*, 326 – 330.
[6] M. Yarmolinsky, L. Gabriel, *Proc. Natl. Acad. Sci. USA* **1959**, *45*, 1721 – 1729.
[7] D. R. Ziehr, J. P. Ellis, P. H. Culviner, S. Cavagnero, *Anal. Chem.* **2010**, *82*, 4637 – 4643.
[8] V. I. Katunin, G. W. Muth, S. A. Strobel, W. Wintermeyer, M. V. Rodnina, *Mol. Cell* **2002**, *10*, 339 – 346.
[9] I. Wohlgemuth, S. Brenner, M. Beringer, M. V. Rodnina, *J. Biol. Chem.* **2008**, *283*, 32229 – 32235.
[10] S. Pestka, *Methods Enzymol.* **1974**, *30*, 470 – 479.
[11] D. Nathans, A. Neidle, *Nature* **1963**, *197*, 1076 – 1077.
[12] S. Starck, R. Roberts, *RNA* **2002**, *8*, 890 – 903.
[13] S. R. Starck, X. Qi, B. N. Olsen, R. W. Roberts, *J. Am. Chem. Soc.* **2003**, *125*, 8090 – 8091.
[14] E. M. Youngman, J. L. Brunelle, A. B. Kochaniak, R. Green, *Cell* **2004**, *117*, 589 – 599.
[15] C. Rodriguez-Fonseca, H. Phan, K. Long, *RNA* **2000**, *6*, 744 – 754.
[16] S.-T. D. Hsu, P. Fucini, L. D. Cabrita, H. Launay, C. M. Dobson, J. Christodoulou, *Proc. Natl. Acad. Sci. USA* **2007**, *104*, 16516 – 16521.
[17] S. R. Starck, H. M. Green, J. Alberola-Ila, R. W. Roberts, *Chem. Biol.* **2004**, *11*, 999 – 1008.
[18] D. K. Eggers, W. J. Welch, W. J. Hansen, *Mol. Biol. Cell* **1997**, *8*, 1559 – 1573.
[19] R. Roberts, J. Szostak, *Proc. Natl. Acad. Sci. USA* **1997**, *94*, 12297 – 12302.
[20] T. Ishizawa, T. Kawakami, P. C. Reid, H. Murakami, *J. Am. Chem. Soc.* **2013**, *135*, 5433 – 5440.
[21] R. Aviner, T. Geiger, O. Elroy-Stein, *Genes Dev.* **2013**, *27*, 1834 – 1844.
[22] N. Umeda, T. Ueno, C. Pohlmeyer, T. Nagano, T. Inoue, *J. Am. Chem. Soc.* **2011**, *133*, 12 – 14.
[23] M. Goard, G. Aakalu, O. D. Fedoryak, C. Quinonez, J. St Julien, S. J. Poteet, E. M. Schuman, T. M. Dore, *Chem. Biol.* **2005**, *12*, 685 – 693.
[24] A. Patchornik, B. Amit, R. Woodward, *J. Am. Chem. Soc.* **1970**, *92*, 6333 – 6335.
[25] C. Bochet, *J. Chem. Soc. Perkin Trans. 1* **2002**, 125 – 142.
[26] J. F. Cameron, J. M. J. Frechet, *J. Am. Chem. Soc.* **1991**, *113*, 4303 – 4313.
[27] E. Pick, O.-S. Lau, T. Tsuge, S. Menon, Y. Tong, N. Dohmae, S. M. Plafker, X. W. Deng, N. Wei, *Mol. Cell. Biol.* **2007**, *27*, 4708 – 4719.
[28] D. A. Grueneberg, W. Li, J. E. Davies, J. Sawyer, J. Pearlberg, E. Harlow, *Proc. Natl. Acad. Sci. USA* **2008**, *105*, 16490 – 16495.
[29] J. Kohl-Landgraf, F. Buhr, D. Lefrancois, J.-M. Mewes, H. Schwalbe, A. Dreuw, J. L. Wachtveitl, *J. Am. Chem. Soc.* **2014**, *136*,3430 – 3438.
[30] T. Kühn, H. Schwalbe, *J. Am. Chem. Soc.* **2000**, *122*, 8856 – 8861.
[31] V. A. Kolb, E. V. Makeyev, A. S. Spirin, *EMBO J.* **1994**, *13*, 3631 – 3637.
[32] A. David, B. P. Dolan, H. D. Hickman, J. J. Knowlton, G. Clavarino, P. Pierre, J. R. Bennink, J. W. Yewdell, *J. Cell Biol.* **2012**, *197*, 45 – 57.
[33] E. K. Schmidt, G. Clavarino, M. Ceppi, P. Pierre, *Nat. Methods* **2009**, *6*, 275 – 277.
[34] C. E. Holt, E. M. Schuman, *Neuron* **2013**, *80*, 648 – 657.
[35] K. C. Martin, A. Ephrussi, *Cell* **2009**, *136*, 719 – 730.

